Eur. Phys. J. C 51, 701–711 (2007)
DOI 10.1140/epjc/s10052-007-0307-6

THE EUROPEAN PHYSICAL JOURNAL C

Regular Article – Theoretical Physics

The Landau pole and Z' decays in the 331 dilepton model

R. Martínez[a], F. Ochoa[b]

Departamento de Física, Universidad Nacional, Bogotá, Colombia

Received: 17 November 2006 / Revised version: 22 February 2007 /
Published online: 3 May 2007 –

Abstract. We calculate the decay widths and branching ratios of the extra neutral boson Z' predicted by the 331 dilepton model in the framework of two different particle contents. These calculations are performed taking into account oblique radiative corrections and flavor changing neutral currents (FCNC) under the ansatz of Matsuda as a texture for the quark mass matrices. Contributions of the order of 10^{-1}–10^{-2} are obtained in the branching ratios, and the partial widths about one order of magnitude bigger in relation with other 331 models are also obtained. A Landau-like pole arises at 3.5 TeV considering the full particle content of the minimal dilepton model (MDM), where the exotic sector is considered as a degenerate spectrum at the 3 TeV scale. The Landau pole problem can be avoided at the TeV scales if a new leptonic content running below the threshold at 3 TeV is implemented as suggested by other authors.

1 Introduction

The models with gauge symmetry $\mathrm{SU}(3)_c \otimes \mathrm{SU}(3)_\mathrm{L} \otimes \mathrm{U}(1)_X$, also called 331 models, arise by enlarging the symmetry group in which the standard model (SM) is embedded as an effective theory at low energy. Based on the criterion of the cancellation of chiral anomalies [1–6], these models have generated new expectations and possibilities of new physics at the TeV scale whose predictions are accessible to experimental observation and will be of great interest in the next generation of colliders (LHC, ILC) [7–9] at the TeV energy scales. One of the most remarkable features of these models is that they arise as an interesting alternative to explain the origin of generations [10]; they lead to the prediction of new neutral and charged vector bosons with observable consequences at low and high energies, and they can predict charge quantization for a three family model even when neutrino masses are added [11, 12].

Although cancellation of anomalies leads to some required conditions [13], such a criterion on its own still permits an infinite number of 331 models. In these models, the electric charge is defined in general as a linear combination of the diagonal generators of the group,

$$Q = T_3 + \beta T_8 + XI\,, \tag{1}$$

where the value of the β parameter determines the fermion assignment and, more specifically, the electric charges of the exotic spectrum. Hence, it is customary to use this quantum number to classify the different 331 models. There are four main versions of 331 models corresponding to $\beta = \pm 1/\sqrt{3}$ [13–17], which leads to non-exotic charges, and $\beta = \pm\sqrt{3}$ [18–22], where the model with $\beta = -\sqrt{3}$ accounts for doubly charged dilepton bosons. An extensive and detailed study of models with arbitrary β have been carried out in [23] for the scalar sector and in [24] for the fermionic and gauge sector.

The group structure of these models leads, along with the SM neutral Z boson, to the prediction of an additional current associated to the extra neutral boson Z'. It is possible to obtain constraints through direct production of the Z' boson (for center-of-mass energy $\sqrt{s} \approx M_{Z'} > M_Z$), where the study of decay widths provides information about possible Z' detection in future experimental measurements. These decay widths are controlled by the $\mathrm{SU}(3)_\mathrm{L} \otimes \mathrm{U}(1)_X$ coupling constants denoted by g_L and g_X, respectively, and which obey the relation

$$\frac{g_X^2}{g_\mathrm{L}^2} = \frac{S_\mathrm{W}^2}{1-(1+\beta^2)S_\mathrm{W}^2}\,, \tag{2}$$

where $S_\mathrm{W} = \sin\theta_\mathrm{W}$ with θ_W the Weinberg angle, and where g_L is the same as the SM coupling of the $\mathrm{SU}(2)_\mathrm{L}$ group. Equation (2) exhibits a Landau-like pole when $S_\mathrm{W}^2(\mu) = 1/(1+\beta^2)$, where the coupling constant g_X becomes infinite, and the models lose their perturbative character at some energy scale μ. In particular, the model with $\beta = -\sqrt{3}$ (the dilepton model) shows a Landau pole when $S_\mathrm{W}^2 = 1/4$ at the scale $\mu \approx 4\,\mathrm{TeV}$, which is close to the bounds associated to the Z' mass predicted by this model [25]. Thus, this version of the 331 models points to a nonperturbative regime at the Z' peak in the sense that the couplings between matter and Z' become unlimitedly strong when S_W^2 evolves to near 1/4, as will

[a] e-mail: remartinezm@unal.edu.co
[b] e-mail: faochoap@unal.edu.co

be observed in Table 5. This problem has already been considered in [26] with and without supersymmetry of the dilepton model. In particular, a possible solution of this puzzle was proposed in [27] by introducing an additional particle content, which changes the behavior of the running Weinberg angle and restores the perturbative feature of the model; this we will call the extended 331 dilepton model (EDM). The new particle content of the EDM consists of three exotic lepton triplets, one exotic scalar triplet and two exotic scalar doublets. In this extended model, the usual exotic particles predicted by the minimal 331 dilepton model (MDM) remains as heavy particles, which are decoupled below the scale μ_{331}, where the symmetry breaking $\mathrm{SU}(3)_{\mathrm{L}} \times \mathrm{U}(1)_X \to \mathrm{SU}(2)_{\mathrm{L}} \times \mathrm{U}(1)_Y$ takes place, so that they are not considered as active degrees of freedom below the Z' energy scale. However, some phenomenological studies estimate that the exotic quarks have a mass in the range 1.5–4 TeV [28], and they could enter as active degree of freedom at the Z' scale.

In this work we study the behavior of the running Weinberg angle for different particle content in the 331 dilepton model ($\beta = -\sqrt{3}$), where the exotic particles define a new threshold energy scale below $M_{Z'}$. Later, we will obtain the partial widths and the branching decays of the Z' boson in the 331 dilepton model for two perturbative particle contents, where the running coupling constants at the $M_{Z'}$ scale is taken into account in agreement with the new particle content. This paper is organized as follows. Section 2 is devoted to a summary of the minimal 331 dilepton model (MDM), and in Sects. 2.1 and 2.2 we describe the behavior of the running Weinberg angle in the MDM. In Sect. 2.3, we indicate the most remarkable features of the extended 331 dilepton model (EDM) in order to obtain a decreasing running Weinberg angle. In Sect. 2.4, we consider a modification of the extended 331 dilepton model (MEDM), where we include the exotic spectrum of the minimal model as an active degree of freedom below the Z' scale. Finally, in Sect. 3 we calculate the partial decays and branching ratios of the Z' boson in the framework of the EDM and MEDM models, where the effects of flavor changing neutral currents (FCNC) and oblique radiative corrections are taken into account.

2 Perturbative and nonperturbative dilepton models

In this section we show the different particle contents in the 331 dilepton model, which control the behavior of the Weinberg angle and the coupling constants with increasing energy. The minimal 331 fermionic structure for three families is shown in Table 1 for the dilepton model, corresponding to $\beta = -\sqrt{3}$, where all leptons transform as $(\mathbf{1}, \mathbf{3}, \mathbf{X}^{\mathrm{L}}_{\ell})$ and $(\mathbf{1}, \mathbf{1}, \mathbf{X}^{\mathrm{R}}_{\ell'})$ under $(\mathrm{SU}(3)_c, \mathrm{SU}(3)_{\mathrm{L}}, \mathrm{U}(1)_X)$, with $\mathbf{X}^{\mathrm{L}}_{\ell}$ and $\mathbf{X}^{\mathrm{R}}_{\ell'}$ the $\mathrm{U}(1)_X$ values associated to the left- and right-handed leptons, respectively, while the quarks transform as $(\mathbf{3}, \mathbf{3}^*, \mathbf{X}^{\mathrm{L}}_{q_{m^*}})$, $(\mathbf{3}^*, \mathbf{1}, \mathbf{X}^{\mathrm{R}}_{q'_{m^*}})$ for the first two families, and $(\mathbf{3}, \mathbf{3}, \mathbf{X}^{\mathrm{L}}_{q_3})$, $(\mathbf{3}^*, \mathbf{1}, \mathbf{X}^{\mathrm{R}}_{q'_3})$ for the third family, where $\mathbf{X}^{\mathrm{L}}_{q_{m^*}}, \mathbf{X}^{\mathrm{L}}_{q_3}$ and $\mathbf{X}^{\mathrm{R}}_{q'_{m^*}}, \mathbf{X}^{\mathrm{R}}_{q'_3}$ correspond to the $\mathrm{U}(1)_X$ values for the left- and right-handed quarks. We denote by $\mathbf{X}^{\mathrm{L}}_{q_3}$ and $\mathbf{X}^{\mathrm{L}}_{q_{m^*}}$ the values associated to the $\mathrm{SU}(3)_{\mathrm{L}}$ space under representation $\mathbf{3}$ and $\mathbf{3}^*$, respectively. The quantum numbers $\mathbf{X}_{\psi}$ for each representation are given in the third column of Table 1, where the definition of the electric charge in (1) has been used, demanding charges of $2/3$ and $-1/3$ for the up- and down-type quarks, respectively, and charges of -1 and 0 for the charged and neutral leptons. We recognize three different possibilities to assign the physical quarks in each family representation as shown in Table 2 [29, 30]. At low energy, the three models from Table 2 are equivalent and there is not any phenomenological feature that allows us to detect differences between them. In fact, they must reduce to the SM, which is an universal family model in $\mathrm{SU}(2)_{\mathrm{L}}$. However,

Table 1. Fermionic content for three generations with $\beta = -\sqrt{3}$. We take $m^* = 1, 2$, and $j = 1, 2, 3$

Representation	Q_{ψ}	X_{ψ}
$q_{m^*\mathrm{L}} = \begin{pmatrix} d_{m^*} \\ -u_{m^*} \\ J_{m^*} \end{pmatrix}_{\mathrm{L}} : \mathbf{3}^*$	$\begin{pmatrix} -1/3 \\ 2/3 \\ -4/3 \end{pmatrix}$	$-1/3$
$d_{m^*\mathrm{R}}; u_{m^*\mathrm{R}}; J_{m^*\mathrm{R}}: \mathbf{1}$	$-1/3; 2/3; -4/3$	$-1/3, 2/3, -4/3$
$q_{3\mathrm{L}} = \begin{pmatrix} u_3 \\ d_3 \\ J_3 \end{pmatrix}_{\mathrm{L}} : \mathbf{3}$	$\begin{pmatrix} 2/3 \\ -1/3 \\ 5/3 \end{pmatrix}$	$2/3$
$u_{3\mathrm{R}}; d_{3\mathrm{R}}; J_{3\mathrm{R}}: \mathbf{1}$	$2/3; -1/3; 5/3$	$2/3, -1/3, 5/3$
$\ell_{j\mathrm{L}} = \begin{pmatrix} \nu_j \\ e_j \\ E_j^+ \end{pmatrix}_{\mathrm{L}} : \mathbf{3}$	$\begin{pmatrix} 0 \\ -1 \\ 1 \end{pmatrix}$	0
$e_{j\mathrm{R}}; E_{j\mathrm{R}}^{-Q_1}$	$-1; 1$	$-1, 1$

Table 2. Three different assignments for the $\mathrm{SU}(3)_\mathrm{L}$ family representation of quarks

Representation A	Representation B	Representation C
$q_{m\mathrm{L}} = \begin{pmatrix} d, s \\ -u, -c \\ J_1, J_2 \end{pmatrix}_\mathrm{L} : \mathbf{3}^*$	$q_{m\mathrm{L}} = \begin{pmatrix} d, b \\ -u, -t \\ J_1, J_3 \end{pmatrix}_\mathrm{L} : \mathbf{3}^*$	$q_{m\mathrm{L}} = \begin{pmatrix} s, b \\ -c, -t \\ J_2, J_3 \end{pmatrix}_\mathrm{L} : \mathbf{3}^*$
$q_{3\mathrm{L}} = \begin{pmatrix} t \\ b \\ J_3 \end{pmatrix}_\mathrm{L} : \mathbf{3}$	$q_{3\mathrm{L}} = \begin{pmatrix} c \\ s \\ J_2 \end{pmatrix}_\mathrm{L} : \mathbf{3}$	$q_{3\mathrm{L}} = \begin{pmatrix} u \\ d \\ J_1 \end{pmatrix}_\mathrm{L} : \mathbf{3}$

through the couplings of the three families to the additional neutral current (Z') and the introduction of a mixing angle between Z and Z', it is possible to recognize differences between the three models at the electroweak scale [25, 31].

For the scalar sector described by Table 3, we introduce the triplet field χ with vacuum expectation value (VEV) $\langle\chi\rangle^\mathrm{T} = (0, 0, \nu_\chi)$, which induces masses to the third fermionic components. In the second transition it is necessary to introduce two triplets ρ and η with VEV $\langle\rho\rangle^\mathrm{T} = (0, \nu_\rho, 0)$ and $\langle\eta\rangle^\mathrm{T} = (\nu_\eta, 0, 0)$ in order to give masses to the quarks of type up and down, respectively.

In the gauge boson spectrum associated with the group $\mathrm{SU}(3)_\mathrm{L} \otimes \mathrm{U}(1)_X$, we have the charged sector

$$W_\mu^\pm = \frac{1}{\sqrt{2}}\left(W_\mu^1 \mp \mathrm{i}W_\mu^2\right); \quad K_\mu^{\pm 1} = \frac{1}{\sqrt{2}}\left(W_\mu^4 \mp \mathrm{i}W_\mu^5\right);$$
$$K_\mu^{\pm 2} = \frac{1}{\sqrt{2}}\left(W_\mu^6 \mp \mathrm{i}W_\mu^7\right), \tag{3}$$

and the neutral sector that corresponds to the photon, the Z and the Z' bosons

$$A_\mu = S_\mathrm{W} W_\mu^3 + C_\mathrm{W}\left(-\sqrt{3}T_\mathrm{W} W_\mu^8 + \sqrt{1 - 3T_\mathrm{W}^2}B_\mu\right),$$
$$Z_\mu = C_\mathrm{W} W_\mu^3 - S_\mathrm{W}\left(-\sqrt{3}T_\mathrm{W} W_\mu^8 + \sqrt{1 - 3T_\mathrm{W}^2}B_\mu\right),$$
$$Z'_\mu = -\sqrt{1 - 3T_\mathrm{W}^2} W_\mu^8 - \sqrt{3}T_\mathrm{W} B_\mu, \tag{4}$$

Table 3. Scalar spectrum that breaks the 331 symmetry and gives masses to the fermions

	Q_Φ	X_Φ
$\chi = \begin{pmatrix} \chi_1^- \\ \chi_2^{--} \\ \xi_\chi + \nu_\chi \pm \mathrm{i}\zeta_\chi \end{pmatrix}$	$\begin{pmatrix} -1 \\ -2 \\ 0 \end{pmatrix}$	-1
$\rho = \begin{pmatrix} \rho_1^+ \\ \xi_\rho + \nu_\rho \pm \mathrm{i}\zeta_\rho \\ \rho_3^{++} \end{pmatrix}$	$\begin{pmatrix} 1 \\ 0 \\ 2 \end{pmatrix}$	1
$\eta = \begin{pmatrix} \xi_\eta + \nu_\eta \pm \mathrm{i}\zeta_\eta \\ \eta_2^- \\ \eta_3^+ \end{pmatrix}$	$\begin{pmatrix} 0 \\ -1 \\ 1 \end{pmatrix}$	0

where the Weinberg angle is defined by

$$S_\mathrm{W} = \sin\theta_\mathrm{W} = \frac{g_X}{\sqrt{g_\mathrm{L}^2 + 4g_X^2}},$$
$$T_\mathrm{W} = \tan\theta_\mathrm{W} = \frac{g_X}{\sqrt{g_\mathrm{L}^2 + 3g_X^2}}. \tag{5}$$

Further, a small mixing angle between the two neutral currents Z_μ and Z'_μ appears with the following mass eigenstates [24]:

$$Z_{1\mu} = Z_\mu C_\theta + Z'_\mu S_\theta; \quad Z_{2\mu} = -Z_\mu S_\theta + Z'_\mu C_\theta;$$
$$\tan\theta = \frac{1}{\Lambda + \sqrt{\Lambda^2 + 1}};$$
$$\Lambda = \frac{-2S_\mathrm{W}C_\mathrm{W}^2 g_X^2 \nu_\chi^2 + \frac{3}{2}S_\mathrm{W}T_\mathrm{W}^2 g_\mathrm{L}^2\left(\nu_\eta^2 + \nu_\rho^2\right)}{g_\mathrm{L} g_X T_\mathrm{W}^2\left[-3\sqrt{3}S_\mathrm{W}^2\left(\nu_\eta^2 + \nu_\rho^2\right) + C_\mathrm{W}^2\left(\nu_\eta^2 - \nu_\rho^2\right)\right]}. \tag{6}$$

On the other hand, the solution of the renormalization group at the lowest one-loop order gives the running coupling constant for $\widetilde{M} \leq \mu$:

$$g_i^{-2}(\widetilde{M}) = g_i^{-2}(\mu) + \frac{b_i}{8\pi^2}\ln\left(\frac{\mu}{\widetilde{M}}\right). \tag{7}$$

Below the breaking scale μ_{331} the subscripts $i = 1, 2, 3$, correspond to the coupling constant of $\mathrm{U}(1)_Y$, $\mathrm{SU}(2)_\mathrm{L}$ and $\mathrm{SU}(3)_c$, respectively. Specifically, we use the matching condition for the coupling constants, where the $\mathrm{SU}(3)_\mathrm{L}$ constant g_L is the same as the $\mathrm{SU}(2)_\mathrm{L}$ constant, i.e. $g_2 = g_\mathrm{L}$. Running the constants at the scale $\mu = M_{Z'}$, we obtain for $g_1 = g_Y$ and $g_2 = g_\mathrm{L}$

$$g_Y^2(M_{Z'}) = \frac{g_Y^2(\widetilde{M})}{1 - \frac{b_1}{8\pi^2}g_Y^2(\widetilde{M})\ln\left(\frac{M_{Z'}}{\widetilde{M}}\right)},$$
$$g_\mathrm{L}^2(M_{Z'}) = \frac{g_\mathrm{L}^2(\widetilde{M})}{1 - \frac{b_2}{8\pi^2}g_\mathrm{L}^2(\widetilde{M})\ln\left(\frac{M_{Z'}}{\widetilde{M}}\right)}, \tag{8}$$

where the renormalization coefficients for a general $\mathrm{SU}(N)$ gauge group are defined by

$$b_i = \frac{2}{3}\sum_\text{fermions}\mathrm{Tr}(T_i(F)T_i(F)) + \frac{1}{3}\sum_\text{scalars}\mathrm{Tr}(T_i(S)T_i(S)) - \frac{11}{3}C_{2i}(G), \tag{9}$$

with $T_i(I)$ corresponding to the generators of the fermionic (F) or scalar (S) representations. For $\mathrm{SU}(N)$,

$\mathrm{Tr}(T(I)T(I)) = 1/2$ and $C_2(G) = N$. For $\mathrm{U}(1)_Y$, $\mathrm{Tr}(T(I)T(I)) = Y^2$ and $C_2(G) = 0$. With the above definitions, we can obtain the running Weinberg angle at the Z' scale:

$$S^2_{\mathrm{W}}(M_{Z'}) = \frac{g^2_Y(M_{Z'})}{g^2_{\mathrm{L}}(M_{Z'}) + g^2_Y(M_{Z'})} = S^2_{\mathrm{W}}(\widetilde{M}) \left[\frac{1 - \frac{b_2}{2\pi}\alpha_{\mathrm{L}}(\widetilde{M}) \ln\left(M_{Z'}/\widetilde{M}\right)}{1 - \frac{b_1+b_2}{2\pi}\alpha(\widetilde{M}) \ln\left(M_{Z'}/\widetilde{M}\right)} \right]. \tag{10}$$

2.1 The effective two Higgs doublet model (THDM)

The running Weinberg angle from (10) depends on the particle content of the model. First, we consider only the particle content of the effective two Higgs doublet model (THDM) below $M_{Z'}$, where the heavy exotic fermions J_{m^*} and J_3 and E_j, the scalar singlets ρ_3^{++} and η_3^+ and the scalar triplet χ in Table 1 are not considered as active degrees of freedom; i.e., they are decoupled below the symmetry breaking scale μ_{331}. Thus, the renormalization coefficient takes the values

$$b_1 = \frac{20}{9}N_f + \frac{1}{6}N_H = 7\,, \qquad b_2 = \frac{4}{3}N_f + \frac{1}{6}N_H - \frac{22}{3} = -3\,, \tag{11}$$

where $N_f = 3$ is the number of fermion families and $N_H = 2$ the number of $\mathrm{SU}(2)_{\mathrm{L}}$ scalar doublets of the effective THDM. Taking $\widetilde{M} = M_Z$ we run (8) and (10) using the following values at the M_Z scale:

$$\begin{aligned} \alpha_Y^{-1}(M_Z) &= 98.36461 \pm 0.06657\,; \\ \alpha^{-1}(M_Z) &= 127.934 \pm 0.027\,; \\ \alpha_{\mathrm{L}}^{-1}(M_Z) &= 29.56938 \pm 0.00068\,; \\ S^2_{\mathrm{W}}(M_Z) &= 0.23113 \pm 0.00015\,, \end{aligned} \tag{12}$$

where we use the usual definition $\alpha_i = g_i^2/4\pi$. Figure 1 displays the evolution of the Weinberg angle for the effective THDM of the minimal 331 dilepton model. We can see a Landau pole at the energy scale $\mu \approx 4$ TeV, which corresponds to the lowest bound of the Z' mass for the dilepton model, as studied in [25]. Then, as shown in [26], perturbation theory cannot be used at the TeV scale energies in the minimal model even though supersymmetry may have been implemented.

2.2 The minimal 331 dilepton model (MDM)

In the previous model, the exotic spectrum of the MDM is considered as heavy particles that are decoupled below the breaking scale μ_{331} and do not participate as an active degree of freedom in the renormalization coefficient. However, by comparing the data with radiative corrections to the decay $Z \to b\bar{b}$ carried out in [28], exotic quarks with a mass in the range 1.5–4 TeV are expected for the 331 dilepton model, which lies in the range below the Z' scale. Then, we take the full 331 spectrum from Tables 1 and 3, where the exotic particles of the MDM are considered as a degenerate spectrum. In agreement with [28], it is reasonable to estimate $m_{J_j, E_j, \rho_3^{++}, \eta_3^+, \chi_1^-, \chi_2^{--}} \approx 3$ TeV, defining a new running scale. Then the Weinberg angle evolves from the Z scale in a two stage process. First, below $\mu = 3$ TeV, the running parameters evolve as described by (10), with the coefficients from (11) of the effective THDM, from which we obtain at 3 TeV

$$\begin{aligned} &\alpha_Y^{-1}(3\ \mathrm{TeV}) = 94.4724\,; \quad \alpha^{-1}(3\ \mathrm{TeV}) = 125.710\,; \\ &\alpha_{\mathrm{L}}^{-1}(3\ \mathrm{TeV}) = 31.2374\,; \quad S^2_{\mathrm{W}}(3\ \mathrm{TeV}) = 0.24849\,. \end{aligned} \tag{13}$$

Later, above the 3 TeV threshold, the spectrum will contain the exotic particles of the minimal model with the following coefficients:

$$b_1 = \frac{20}{9}N_f + \frac{1}{6}N_H + \frac{2}{3}\sum_{\text{sing.}} Y_f^2 + \frac{1}{3}\sum_{\text{sing}} Y_s^2 + \frac{2}{3}Y_\chi^2 = \frac{79}{2}\,, \qquad b_2 = \frac{4}{3}N_f + \frac{1}{6}N_H - \frac{43}{3} = -\frac{17}{6}\,, \tag{14}$$

with $Y_{f,s}$ the hypercharge of the singlets $f = J_j, E_j$ and $s = \rho_3^{++}, \eta_3^+$, and Y_χ is the hypercharge of the doublet (χ_1^-, χ_2^{--}). For the second stage, we apply again (10), but with the inputs at $\widetilde{M} = 3$ TeV from (13). In this way, we obtain the plot shown in Fig. 2. We can see how the behavior of the running angle changes at the 3 TeV scale. The direct consequence of unloading the exotic spectrum

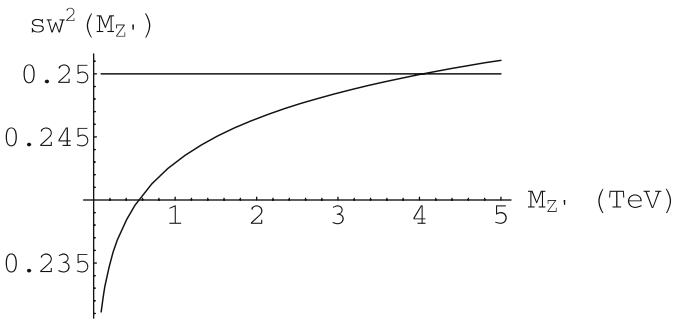

Fig. 1. Running Weinberg angle for the effective THDM of the minimal 331 dilepton model. A Landau-like pole is found at the $M_{Z'} \approx 4$ TeV energy scale

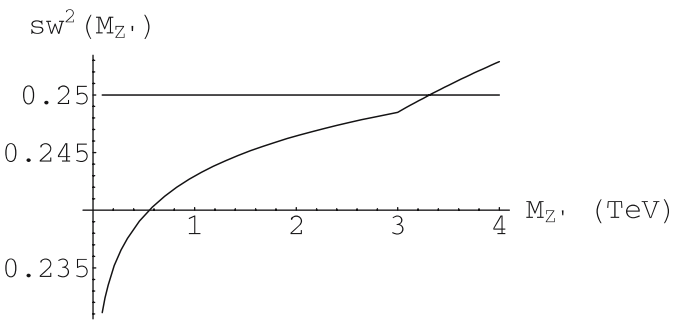

Fig. 2. Running Weinberg angle for the MDM, including the exotic particles at the 3 TeV threshold below $M_{Z'}$. A Landau-like pole is found at 3.5 TeV energy scale

of the MDM below $M_{Z'}$ ($3\,\text{TeV} < M_{Z'}$) is that the Weinberg angle increases faster and reaches the Landau pole at 3.5 TeV below the Z' scale, as observed in Fig. 2.

2.3 The extended 331 dilepton model (EDM)

In order to avoid the nonperturbative character of the dilepton model at the TeV energies, it was proposed in [27] to introduce an additional exotic particle content, where three lepton triplets with null hypercharge, one scalar triplet with null hypercharge and two scalar doublets with $Y^2 = 9$ remain as new degrees of freedom at energies below the scale μ_{331} in order to obtain a perturbative regime at the Z' energy scale, while the minimal exotic spectrum J_j, E_j, ρ_3^{++}, η_3^{+}, χ_1^{-}, χ_2^{--} are preserved as inactive degrees of freedom. In this case, the renormalization coefficients take the form

$$b_1 = \frac{20}{9}N_f + \frac{1}{6}N_H + \frac{Y_{\rm S}^2}{6}N_{\rm S} + Y_{\rm TF}^2 N_{\rm TF} + \frac{Y_{\rm TS}^2}{4}N_{\rm TS} = 10\,,$$
$$b_2 = \frac{4}{3}N_f + \frac{1}{6}N_H - \frac{22}{3} + \frac{8}{3}N_{\rm TF} + \frac{2}{3}N_{\rm TS} + \frac{1}{6}N_{\rm S} = 6\,, \tag{15}$$

with $N_{\rm S} = 2$ the number of new scalar doublets, $N_{\rm TF} = 3$ the number of new fermionic triplets, and $N_{\rm TS} = 1$ the number of new scalar triplets, each one with the corresponding hypercharge values $Y_{\rm S} = \pm 3$, $Y_{\rm TF} = 0$ and $Y_{\rm TS} = 0$. In this case, the Weinberg angle runs as shown by Fig. 3 [27], exhibiting a decreasing behavior at the TeV scale. Thus the perturbative character of the model is restored. The new particles are embedded in three octet representations for leptons and one octet for the scalar sector. Thus, there are additional new leptons, which can be made heavy through the scalar octet. The $\mathrm{U}(1)_X$ quantum number of these new multipets are null, so that they do not contribute to the anomalies and the cancellation of anomalies is preserved. Table 4 resumes the new bunch of particles of the EDM.

2.4 Modification to the extended 331 dilepton model (MEDM)

In the above extended model, the exotic spectrum of the MDM in Table 1 is not considered. However, as it was noted in Sect. 2.2, it is reasonable to introduce this sector above the 3 TeV scale. In this case, the evolution of the coupling constant is controlled by the coefficients in (15), from which we get the new inputs at the threshold

$$\alpha_Y^{-1}(3\,\text{TeV}) = 92.8048\,; \quad \alpha^{-1}(3\,\text{TeV}) = 119.038\,;$$
$$\alpha_{\rm L}^{-1}(3\,\text{TeV}) = 26.2334\,; \quad S_{\rm W}^2(3\,\text{TeV}) = 0.22038\,. \tag{16}$$

Above 3 TeV, the full exotic spectrum of the MDM is activated, and the renormalization coefficients are defined as the combination of (14) and (15), so that we obtain $b_1 = 85/2$ and $b_2 = 37/6$. We see in this case that the Landau pole is pulled to very high scales, as we can observe in Fig. 4, where the Weinberg angle decreases with energy until the 3 TeV threshold, from where it begins to increase slowly so that perturbation theory can be applied at the Z' scale. Thus, the Landau pole is pulled beyond the TeV energy scales.

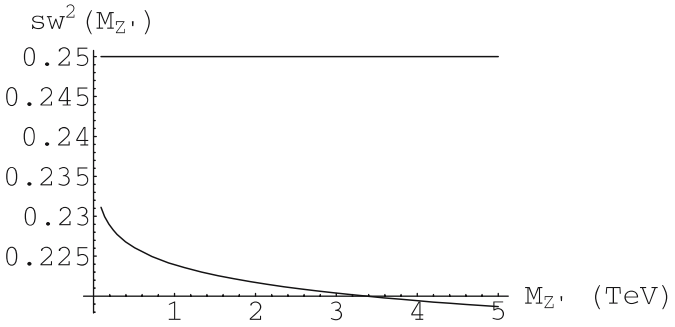

Fig. 3. Running Weinberg angle for the extended 331 dilepton model (EDM) with a new set of leptonic particles. The angle shows a decreasing behavior, from where the Landau pole is avoided

Table 4. Additional particle content in the extended 331 dilepton model (EDM), with $a = 1, 2, 3$ in the lepton sector

	Representation
Leptons	$\Xi_{\rm a} = \begin{pmatrix} \frac{1}{\sqrt{2}}t_{\rm a}^0 + \frac{1}{\sqrt{6}}\lambda_{\rm a}^0 & t_{\rm a}^+ & \delta_{\rm a}^- \\ t_{\rm a}^- & \frac{-1}{\sqrt{2}}t_{\rm a}^0 + \frac{1}{\sqrt{6}}\lambda_{\rm a}^0 & \delta_{\rm a}^{--} \\ \xi_{\rm a}^+ & \xi_{\rm a}^{++} & \frac{-2}{\sqrt{6}}\lambda_{\rm a}^0 \end{pmatrix}$
Scalars	$\Sigma = \begin{pmatrix} \frac{1}{\sqrt{2}}\phi^0 + \frac{1}{\sqrt{6}}\varphi^0 & \phi^+ & \varphi_1^- \\ \phi^- & \frac{-1}{\sqrt{2}}\phi^0 + \frac{1}{\sqrt{6}}\varphi^0 & \varphi_1^{--} \\ \varphi_2^+ & \varphi_2^{++} & \frac{-2}{\sqrt{6}}\varphi^0 \end{pmatrix}$

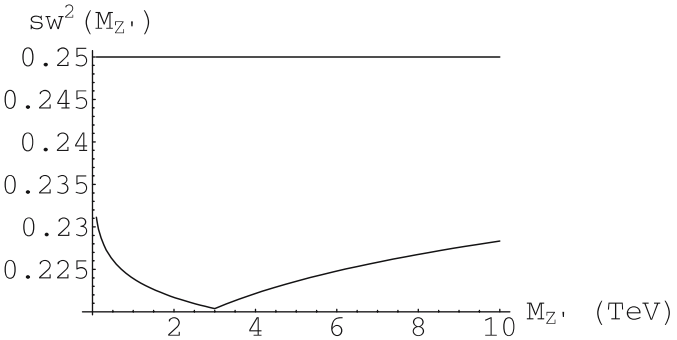

Fig. 4. Running Weinberg angle after modifying the extended dilepton model (MEDM) with the exotic particles of the MDM defined at the 3 TeV threshold. A Landau-like pole is pulled far away from the TeV energy scales

3 The Z' decays in the perturbative models

In this section, we obtain the Z' decay for the dilepton model in the frameworks of two different particle contents.

In Table 2, which is written in the weak eigenstates $f^{0(r)}$, we consider linear combinations in each representation $r = A, B, C$ among the three families to obtain the

couplings in the mass eigenstates $f^{(r)}$ through the rotation matrix R_f that diagonalizes the Yukawa mass terms, where $f^{0(r)} = R_f f^{(r)}$. Thus, the neutral couplings associated with Z' and the SM fermions in the mass eigenstates can be written as [31]

$$\begin{aligned}\mathcal{L}^{\rm NC} = \frac{g_{\rm L}}{2C_{\rm W}}\big\{ &\big[\overline{U}\gamma_\mu\big(\tilde{\mathfrak{g}}_{\rm v}^{{\rm U}(r)} - \tilde{\mathfrak{g}}_{\rm a}^{{\rm U}(r)}\gamma_5\big)U \\ &+ \overline{D}\gamma_\mu\big(\tilde{\mathfrak{g}}_{\rm v}^{D(r)} - \tilde{\mathfrak{g}}_{\rm a}^{D(r)}\gamma_5\big)D + \overline{N}\gamma_\mu\big(\tilde{g}_{\rm v}^{N} - \tilde{g}_{\rm a}^{N}\gamma_5\big)N \\ &+ \overline{E}\gamma_\mu\big(\tilde{g}_{\rm v}^{E} - \tilde{g}_{\rm a}^{E}\gamma_5\big)E\big]Z'^{\mu}\big\}\,, \end{aligned} \tag{17}$$

with $U = (u, c, t)^{\rm T}$, $D = (d, s, b)^{\rm T}$, $N = (\nu_e, \nu_\mu, \nu_\tau)^{\rm T}$, $E = (e, \mu, \tau)^{\rm T}$, and $\tilde{\mathfrak{g}}_{v,a}^{q(r)} = R_q^\dagger \tilde{g}_{v,a}^{q(r)} R_q$. Thus, we obtain flavor changing couplings in the quark sector due to the matrix R_f. The vector and axial vector couplings of the Z' field are listed in Table 5 for each component.

In general, the low energy limit of the 331 models is equivalent to the THDM type III [31–39], which exhibits FCNC due to the non-diagonal components of the Yukawa couplings. In order to avoid fine-tuning, we adopt the ansatz of Matsuda [40] on the texture of the quark mass matrices with the following rotation matrices:

$$R_D = \begin{pmatrix} c & s & 0 \\ -\frac{s}{\sqrt{2}} & \frac{c}{\sqrt{2}} & -\frac{1}{\sqrt{2}} \\ -\frac{s}{\sqrt{2}} & \frac{c}{\sqrt{2}} & \frac{1}{\sqrt{2}} \end{pmatrix}; \quad R_U = \begin{pmatrix} c' & 0 & s' \\ -\frac{s'}{\sqrt{2}} & -\frac{1}{\sqrt{2}} & \frac{c'}{\sqrt{2}} \\ -\frac{s'}{\sqrt{2}} & \frac{1}{\sqrt{2}} & \frac{c'}{\sqrt{2}} \end{pmatrix}, \tag{18}$$

with

$$\begin{aligned} c &= \sqrt{\frac{m_s}{m_d + m_s}}\,; & s &= \sqrt{\frac{m_d}{m_d + m_s}}\,; \\ c' &= \sqrt{\frac{m_t}{m_t + m_u}}\,; & s' &= \sqrt{\frac{m_u}{m_t + m_u}}\,, \end{aligned} \tag{19}$$

where the quark masses at the $M_{Z'}$ scale are (see Appendix B)

$$\begin{aligned} \overline{m_u}(M_{Z'}) &= 0.00170\,{\rm GeV}\,; \\ \overline{m_c}(M_{Z'}) &= 0.509\,{\rm GeV}\,; \\ \overline{m_t}(M_{Z'}) &= 142.579\text{–}142.592\,{\rm GeV}\,; \\ \overline{m_d}(M_{Z'}) &= 0.00342\,{\rm GeV}\,; \\ \overline{m_s}(M_{Z'}) &= 0.0682\,{\rm GeV}\,; \\ \overline{m_b}(M_{Z'}) &= 2.317\,{\rm GeV}\,, \end{aligned} \tag{20}$$

where the two values of $\overline{m_t}(M_{Z'})$ correspond to the MEDM model and the EDM model, respectively. The masses of the other quarks do not exhibit appreciable differences between both models. The above rotation matrices will induce significant FCNC effects at low energies in parameters such as the particle–antiparticle mixing in meson systems, which have been experimentally determined. In particular, our texture prescription fits into the experimental bounds if $M_{Z'}$ is constrained to be bigger than a few TeV values in D_0–$\overline{D_0}$ mixing to various tens of TeV in B_s–$\overline{B_s}$ mixing. Thus, these low energy fits may require a bound of $M_{Z'}$ bigger than 4 TeV. Since the experimental measurement of some of the above mixings still exhibits high levels of errors, we suppose that the FCNC predictions at high energy with the Matsuda ansatz will lead to reasonable values. Detailed studies in the K_0–$\overline{K_0}$, D_0–$\overline{D_0}$ and B_0–$\overline{B_0}$ systems in the context of 331 models have been carried out in [41, 42].

Table 5. Vector and axial vector couplings of fermions and Z' boson

Fermion	$\tilde{g}_{\rm v}^f$	$\tilde{g}_{\rm a}^f$
ν_j	$\frac{-\sqrt{1-4S_{\rm W}^2}}{2\sqrt{3}}$	$\frac{-\sqrt{1-4S_{\rm W}^2}}{2\sqrt{3}}$
e_j	$\frac{-1+10S_{\rm W}^2}{2\sqrt{3}\sqrt{1-4S_{\rm W}^2}}$	$\frac{-\sqrt{1-4S_{\rm W}^2}}{2\sqrt{3}}$
E_j	$\frac{1-5S_{\rm W}^2}{\sqrt{3}\sqrt{1-4S_{\rm W}^2}}$	$\frac{1-S_{\rm W}^2}{\sqrt{3}\sqrt{1-4S_{\rm W}^2}}$
d_{m^*}	$\frac{1}{2\sqrt{3}\sqrt{1-4S_{\rm W}^2}}$	$\frac{\sqrt{1-4S_{\rm W}^2}}{2\sqrt{3}}$
u_{m^*}	$\frac{1-6S_{\rm W}^2}{2\sqrt{3}\sqrt{1-4S_{\rm W}^2}}$	$\frac{1+2S_{\rm W}^2}{2\sqrt{3}\sqrt{1-4S_{\rm W}^2}}$
J_{m^*}	$\frac{-1+9S_{\rm W}^2}{\sqrt{3}\sqrt{1-4S_{\rm W}^2}}$	$\frac{-1+S_{\rm W}^2}{\sqrt{3}\sqrt{1-4S_{\rm W}^2}}$
u_3	$\frac{-1-4S_{\rm W}^2}{2\sqrt{3}\sqrt{1-4S_{\rm W}^2}}$	$\frac{-\sqrt{1-4S_{\rm W}^2}}{2\sqrt{3}}$
d_3	$\frac{-1+2S_{\rm W}^2}{2\sqrt{3}\sqrt{1-6S_{\rm W}^2}}$	$\frac{-1-2S_{\rm W}^2}{2\sqrt{3}\sqrt{1-4S_{\rm W}^2}}$
J_3	$\frac{1-11S_{\rm W}^2}{\sqrt{3}\sqrt{1-4S_{\rm W}^2}}$	$\frac{1-S_{\rm W}^2}{\sqrt{3}\sqrt{1-4S_{\rm W}^2}}$

3.1 Z' decays in the extended model

To calculate the decay widths, we must include the additional exotic spectrum of the model from Sect. 2.3 in order to have a perturbative model at the required energy level. The partial decay widths of Z' into fermions $f\bar{f}$ at tree level are described by [43–45]

$$\begin{aligned}\Gamma^0_{Z'\to\bar{f}f} = &\frac{g_{\rm L}^2 M_{Z'} N_c^f}{48\pi C_{\rm W}^2}\sqrt{1-\mu_f'^2} \\ &\times\left[\left(1+\frac{\mu_f'^2}{2}\right)\big(\tilde{g}_{\rm v}^f\big)^2 + \big(1-\mu_f'^2\big)\big(\tilde{g}_{\rm a}^f\big)^2\right] R_{\rm QED} R_{\rm QCD}\,, \end{aligned} \tag{21}$$

where $N_c^f = 1, 3$ for leptons and quarks, respectively; $R_{\rm QED,QCD}$ are global final-state QED and QCD corrections, and $\mu_f'^2 = 4m_f^2/M_{Z'}^2$ takes into account kinematical corrections that are only important for the top quark. In order to calculate the corrections $R_{\rm QED,QCD}$ defined in Appendix B, we use the running QED (α) and QCD ($\alpha_{\rm s}$) constants at the $M_{Z'}$ scale [31, 46]. We can also generate Z' decays into different flavors of quarks through the La-

grangian in (17), where at tree level

$$\Gamma^0_{Z'\to qq'} = \frac{g_{\rm L}^2 M_{Z'}}{16\pi C_{\rm W}^2}\left[\left(\tilde{\mathfrak{g}}_{\rm v}^{qq'}\right)^2 + \left(\tilde{\mathfrak{g}}_{\rm a}^{qq'}\right)^2\right] R_{\rm QED} R_{\rm QCD}\,. \quad (22)$$

The decays into the minimal exotic particles $Z' \to K^+K^-$, $K^{++}K^{--}$, $\eta_3^+\eta_3^-$, $\rho_3^{++}\rho_3^{--}$, J_j, E_j are suppressed, because in this case we assume that only the effective THDM contributes, while the exotic particles are taken as heavy particles that are decoupled at energies below the scale μ_{331}, as is noted in Sect. 2.3. Decays into light bosons, $Z' \to h^0h^0$, $Z_1\gamma$, Z_1Z_1, Z_1h^0, W^+W^-, which include the like-SM Higgs boson h^0 of the effective THDM are possible only through the small Z–Z' mixing angle θ defined by (6), so that they are very suppressed and do not contribute to the branching ratios in a significant amount [47]. We do not take these decays into account in our analysis. On the other hand, since the oblique corrections are virtual processes sensitive to the heavy particles at any energy scale, we must consider the one-loop corrections to the Z' decay due to the exotic quarks J_j and leptons E_j at the scale $\mu_{331} \gtrsim M_{Z'}$. In the $\overline{MS}$ scheme, the finite terms of the self-energies contribute to the corrections, which are shown in Appendix A, where the Z' self-energy $\Sigma_{Z'Z'}$, the Z'–Z vacuum polarization $\Pi_{Z'Z}$, and the Z'–photon vacuum polarization $\Pi_{Z'\gamma}$ (see the expressions in Appendix A) lead to the following decay width:

$$\Gamma_{Z'\to\bar{f}f} = \Gamma^0_{Z'\to\bar{f}f}\left(1-\Delta'_f\right), \quad (23)$$

with

$$\Delta'_f \approx \frac{2\left(\tilde{g}_{\rm v}^f \Delta\tilde{g}_{\rm v}^f + \tilde{g}_{\rm a}^f \Delta\tilde{g}_{\rm a}^f\right)}{\left(\tilde{g}_{\rm v}^f\right)^2 + \left(\tilde{g}_{\rm a}^f\right)^2}, \quad (24)$$

which contains the oblique radiative corrections in $\Delta\tilde{g}^f_{\rm v,a}$, which are defined as [31]

$$\begin{aligned}\Delta\tilde{g}_{\rm v}^f &\approx 2S_{\rm W}C_{\rm W}Q_f\Pi_{Z'\gamma}\left(M^2_{Z'}\right)\\ &\quad + g_{\rm v}^f\Pi_{Z_2Z_1}\left(M^2_{Z'}\right)\left(1+\frac{M_Z^2}{M^2_{Z'}}\right)+\frac{1}{2}\tilde{g}_{\rm v}^f\Sigma'_{Z'Z'}\left(M^2_{z_2}\right),\\ \Delta\tilde{g}_{\rm a}^f &\approx g_{\rm a}^f\Pi_{Z'Z}\left(M^2_{Z'}\right)\left(1+\frac{M_Z^2}{M^2_{Z'}}\right)+\frac{1}{2}\tilde{g}_{\rm a}^f\Sigma'_{Z'Z'}\left(M^2_{Z'}\right),\end{aligned} \quad (25)$$

where $\Sigma'_{Z'Z'} = {\rm d}\Sigma_{Z'Z'}/{\rm d}M^2_{Z'}$. The FCNC also exhibit corrections due to the Z' self-energy, where

$$\Gamma_{Z'\to qq'} = \Gamma^0_{Z'\to qq'}\left(1-\Delta'_{qq'}\right), \quad (26)$$

with

$$\Delta'_{qq'} \approx \frac{2\left(\tilde{g}_{\rm v}^{qq'}\Delta\tilde{g}_{\rm v}^{qq'} + \tilde{g}_{\rm a}^{qq'}\Delta\tilde{g}_{\rm a}^{qq'}\right)}{\left(\tilde{g}_{\rm v}^{qq'}\right)^2 + \left(\tilde{g}_{\rm a}^{qq'}\right)^2}, \quad (27)$$

and

$$\Delta\tilde{g}_{\rm v,a}^{qq'} \approx \frac{1}{2}\tilde{g}_{\rm v,a}^{qq'}\Sigma'_{Z'Z'}\left(M^2_{Z'}\right). \quad (28)$$

Here we include only one-loop corrections due to the vacuum polarization, which contribute as $(M_{J,E}/M_{Z'})^2$, and this represents about 1%–4% of the correction as studied in [31]. We are not considering vertex corrections, like for example one-loop corrections to the $b\bar{b}Z'$ vertex through the heavy $K^\pm$ boson, where a contribution of the form $(M_J/M_{K^\pm})^2$, which is lower than the vacuum polarization value, is expected. Thus, we do not expect a significant contribution due to the vertex correction. With the above considerations, and taking into account the running coupling constants at the Z' resonance, we calculate the decay widths. Using (8) and (10) with the renormalization coefficients from (15) of the EDM and the inputs from (12), we get at the $M_{Z'} \approx 4$ TeV scale the result that (see Appendix B)

$$\begin{aligned}\alpha_Y^{-1}(M_{Z'}) &= 92.3468\,; & \alpha^{-1}(M_{Z'}) &= 118.305\,;\\ \alpha_{\rm L}^{-1}(M_{Z'}) &= 25.9587\,; & \alpha_{\rm s}(M_{Z'}) &= 0.0779\,,\\ \overline{m_t}(M_{Z'}) &= 142.592\,{\rm GeV}\,; & S^2_{\rm W}(M_{Z'}) &= 0.2194\,. \end{aligned} \quad (29)$$

With the above values and considering $M_{J_j,E_j} = \mu_{331} \approx M_{Z'} = 4$ TeV, we obtain the widths shown in Table 6 from (23) and in Table 7 for the FCNC contributions from (26). In the first case, values independent on the family representation (universality of family) are obtained for the leptonic sector in the two final rows in the table. In regard to the quark widths, we obtain the family dependent decays shown, so that we identify three dilepton models with the same particle content, but with observ-

Table 6. Partial widths and branching ratios of Z' into fermions at one loop level for each representation A, B, and C, in the framework of the EDM. Leptons have universality of family

	Γ_{ff} (GeV)			$\mathrm{Br}(Z'\to ff)\times 10^{-2}$		
	A	B	C	A	B	C
$u\bar{u}$	73.862	73.862	119.967	13.622	13.635	25.891
$c\bar{c}$	73.862	119.967	73.862	13.622	22.146	15.940
$t\bar{t}$	119.962	73.325	73.325	22.124	13.536	15.825
$d\bar{d}$	34.211	34.211	81.097	6.309	6.315	17.502
$s\bar{s}$	34.211	81.097	34.211	6.309	14.971	7.383
$b\bar{b}$	81.097	34.211	34.211	14.956	6.315	7.383
$\ell^+\ell^-$		38.732		7.143	7.150	8.359
$\nu\bar{\nu}$		0.308		0.057	0.057	0.066

Table 7. Partial width of Z' into quarks with FCNC for each representation A, B, and C, in the framework of the EDM

$\Gamma_{qq'}$ (GeV)	A, B	C
$Z' \to u\bar{c}$	5.00×10^{-4}	0
$Z' \to u\bar{t}$	5.00×10^{-4}	2.00×10^{-3}
$Z' \to c\bar{t}$	42.05	0
$Z' \to d\bar{s}$	1.91	7.65
$Z' \to d\bar{b}$	2.01	0
$Z' \to s\bar{b}$	40.02	0

Table 8. Partial width of Z' into quarks with FCNC for each representation A, B, and C for the MEDM

$\Gamma_{qq'}$ (GeV)	A, B	C
$Z' \to u\bar{c}$	5.20×10^{-4}	0
$Z' \to u\bar{t}$	5.20×10^{-4}	2.53×10^{-3}
$Z' \to c\bar{t}$	43.63	0
$Z' \to d\bar{s}$	1.98	9.36
$Z' \to d\bar{b}$	2.08	0
$Z' \to s\bar{b}$	41.51	0

able differences. We also obtain the branching ratios of each decay, where we assume that only decays to SM particles are allowed, which is a reasonable approximation, since the other two body decays are very suppressed. In the FCNC contributions, we obtain very small values for decay into the quarks uc and ut. However, we obtain the result that the flavor changing decay into the quarks ct and sb for models A and B are of about the same order of magnitude as the diagonal components in Table 6, so that they contribute to the branching ratios. On the other hand, model C suppresses most of the flavor changing effects of the neutral currents, which is also observed in models with $\beta = 1/\sqrt{3}$ [31]. (Studies on the FCNC in the 331 models were also carried out in [47–57].)

3.2 Z' decays in the MEDM model

Now we calculate the decay widths in the framework of the MEDM from Sect. 2.4. However, we must take into account the new threshold defined by the exotic quarks J_j at 3 TeV, which modify the running QCD constant and the mass of the top quark at the Z' scale. Thus, with the inputs from (16), we obtain at $M_{Z'} \approx 4$ TeV

$$\begin{aligned} &\alpha_Y^{-1}(M_{Z'}) = 67.229\,; && \alpha^{-1}(M_{Z'}) = 101.377\,; \\ &\alpha_L^{-1}(M_{Z'}) = 22.5224\,; && \alpha_s(M_{Z'}) = 0.0791\,, \\ &\overline{m_t}(M_{Z'}) = 142.579\,\text{GeV}\,; && S_W^2(M_{Z'}) = 0.2222\,. \end{aligned} \quad (30)$$

Comparing with (29), we note the dependence of the running constants and top mass on the particle content. The running masses of the other quarks do not present an appreciable change with respect to the values given by (20). Taking into account the one-loop corrections with $M_{J_j,E_j} = 3$ TeV, we obtain the widths from (23) and the branching ratios shown in Table 9. Although the decays $Z_2 \to K^+K^-$, $K^{++}K^{--}$, $\eta_3^+\eta_3^-$, $\rho_3^{++}\rho_3^{--}$ and J_j, E_j are not forbidden if we consider the whole exotic spectrum at the TeV scale, they are very suppressed by kinematical factors [47]. Table 8 shows the FCNC widths for this case.

3.3 Discussion

The results of the decay widths and branching ratios show observable differences between the representations A, B and C; thus, each case from Table 2 defines three models that lead to different predictions of the extra neutral boson Z'. The assignment of the phenomenological quarks to the 331 representations define three different dilepton models with the same particle content.

Comparing the above results with other estimations performed in the framework of models with $\beta = 1/\sqrt{3}$ [31] and dilepton models at tree level [47], we get partial widths about one order of magnitude bigger for the quark sector and the charged lepton sector, while for the neutrinos the results are one order of magnitude smaller. These differences in the partial widths may be used in order to distinguish which 331 model could describe in a better way the

Table 9. Partial widths and branching ratios of Z' into fermions at one loop level for each representation A, B, and C, in the framework of the MEDM. Leptons have universality of family

	Γ_{ff} (GeV)			$\text{Br}(Z' \to ff) \times 10^{-2}$		
	A	B	C	A	B	C
$u\bar{u}$	78.770	78.770	128.91	13.660	13.672	25.974
$c\bar{c}$	78.770	128.91	78.770	13.660	22.375	15.872
$t\bar{t}$	128.90	78.200	78.200	22.353	13.573	15.757
$d\bar{d}$	36.597	36.597	85.817	6.346	6.352	17.292
$s\bar{s}$	36.597	85.817	36.597	6.346	14.895	7.374
$b\bar{b}$	85.817	36.597	36.597	14.882	6.352	7.374
$\ell^+\ell^-$		41.733		7.237	7.243	8.409
$\nu\bar{\nu}$		0.310		0.054	0.054	0.062

physics at the TeV energy scale in future experiments. The branching ratios are in the range $10^{-2} \leq \mathrm{Br}(Z_2 \to qq) \leq 10^{-1}$ for the quarks, $\mathrm{Br}(Z_2 \to \ell^+\ell^-) \approx 10^{-2}$ for the charged leptons, and $\mathrm{Br}(Z_2 \to \nu\nu) \approx 10^{-4}$ for the neutrinos. Comparing with the model $\beta = 1/\sqrt{3}$ [31] or the dilepton model from [47], we get branching ratios between one and two orders of magnitude smaller.

On the other hand, by comparing Tables 6 and 9, we get the result that the MEDM model predicts widths about 6% bigger than the extended model. In general, we see that each decay width increases with exotic particles, in particular when the exotic quarks of the minimal dilepton model are unloaded below the Z' resonance. The branching ratios present very similar values for both particle contents, so that the additional effects of the new threshold and the presence of additional exotic particles are canceled in the calculations of the ratios. Just as the top quark contributes to the one-loop Z decay, the above decay widths were calculated at one-loop level through the heavy particles J_j and E_j, where we take into account the running coupling constant at the $M_{Z'}$ energy level.

The branching ratios receive important contributions to the flavor changing decays $Z' \to ct, sb$ in models A and B. The other flavor changing effects are very small; in particular, the FCNC phenomenology is practically absent for model C, as can be seen in Tables 7 and 8.

4 Conclusions

In this work we studied the main contributions of the Z' decay in the framework of the 331 dilepton model with extra particles that pull the Landau pole beyond energies at the TeV scale in order to get a perturbative model at the Z' peak. These calculations were performed for two different particle contents, first in the extended model proposed in [27], in which three lepton triplets with null hypercharge, one scalar triplet with null hypercharge and two scalar doublets with $Y^2 = 9$ remain as new degrees of freedom at energies below $M_{Z'}$, and later modifying the extended model (MEDM) where the full 331 spectrum from Tables 1 and 3 is taken into account with a degenerate exotic spectrum at 3 TeV in agreement with some phenomenological studies [28]. In particular, the presence of the exotic quarks J_j as an active degree of freedom below the Z' scale define a new threshold that changes the evolution of the running parameters. In general, we obtained predictions for six different perturbative models with two particle contents. As seen in Tables 6–8, each of the cases A, B and C from Table 2 leads to different predictions of the Z' decays; thus, they represent three different dilepton models. The decay widths obtained are of the order of 10^2 GeV for quarks and charged leptons that are one order of magnitude bigger than the ones predicted by the models with $\beta = 1/\sqrt{3}$, while the decays into neutrinos are of the order of 10^{-1} GeV, one order of magnitude smaller than in models $\beta = 1/\sqrt{3}$. We also obtained the branching ratios, where decays into exotic particles are not taken into account for kinematical reasons, and decays into light bosons are suppressed by the small Z–Z' mixing angle. However, FCNC effects through the ansatz of Matsuda on the texture of the quark mass matrices lead to an important contribution in the decays $Z' \to ct, sb$, which are of the order of 10^2 GeV and should be taken into account in the total decay width.

Acknowledgements. We acknowledge financial support from Colciencias. We also thank the HELEN (High Energy Physics Latin American–European Network) Program.

Appendix A: Radiative corrections

The correction due to the Z' self-energy leads to the wave-function renormalization

$$Z' \to Z'_{\mathrm{R}} \approx \left(1 - \frac{1}{2}\Sigma^{(\mathrm{fin})\prime}_{Z'Z'}(q^2)\right) Z' \,, \tag{A.1}$$

which is sensitive to the heavy fermions $f_j = J_j, E_j$, where

$$\begin{aligned}\Sigma^{(\mathrm{fin})\prime}_{Z'Z'}(q^2) &= \frac{\mathrm{d}\,\Sigma^{(\mathrm{fin})}_{Z'Z'}}{\mathrm{d}q^2} \\ &= \frac{1}{12\pi^2}\left(\frac{g_{\mathrm{L}}}{2C_{\mathrm{W}}}\right)^2 \sum_{f_j}\left\{\left(\tilde{g}^{f_j}_{\mathrm{v}}\right)^2\left(\frac{2}{3} - \ln\frac{m^2_{f_j}}{q^2}\right)\right. \\ &\quad \left. + \left(\tilde{g}^{f_j}_{\mathrm{a}}\right)^2\left(\frac{2}{3} - \ln\frac{m^2_{f_j}}{q^2} - \frac{6m^2_{f_j}}{q^2}\right)\right\}. \end{aligned} \tag{A.2}$$

The Z'–Z self-energy leads to the following vacuum polarization:

$$\begin{aligned}\Pi^{(\mathrm{fin})}_{Z'Z}(q^2) \approx \frac{1}{12\pi^2}\left(\frac{g_{\mathrm{L}}}{2C_{\mathrm{W}}}\right)^2 \sum_{f_j}\left\{\tilde{g}^{f_j}_{\mathrm{v}} g^{f_j}_{\mathrm{v}}\left[-\ln\frac{m^2_{f_j}}{q^2} - \frac{1}{3}\right]\right. \\ \left. + \tilde{g}^{f_j}_{\mathrm{a}} g^{f_j}_{\mathrm{a}}\left[\left(\frac{6m^2_{f_j}}{q^2} - 1\right)\ln\frac{m^2_{f_j}}{q^2} - \frac{1}{3}\right]\right\}, \end{aligned} \tag{A.3}$$

and the Z'–photon vacuum polarization is given by

$$\Pi^{(\mathrm{fin})}_{Z'\gamma}(q^2) \approx \frac{1}{12\pi^2}\frac{g^2_{\mathrm{L}} S_{\mathrm{W}}}{2C_{\mathrm{W}}}\sum_{f_j}\left\{Q_{f_j}\tilde{g}^{f_j}_{\mathrm{v}}\left[-\ln\frac{m^2_{f_j}}{q^2} - \frac{1}{3}\right]\right\}, \tag{A.4}$$

with Q_{f_j} the electric charge of the virtual f_j fermions given in Table 1.

Appendix B: Running masses

The Z' decay in (21) contains global QED and QCD corrections through the definition of $R_{\mathrm{QED}} = 1 + \delta^f_{\mathrm{QED}}$ and $R_{\mathrm{QCD}} = 1 + (1/2)(N^f_c - 1)\delta^f_{\mathrm{QCD}}$, where [43–45]

$$\begin{aligned}\delta^f_{\mathrm{QED}} &= \frac{3\alpha Q^2_f}{4\pi}\,; \\ \delta^f_{\mathrm{QCD}} &= \frac{\alpha_{\mathrm{s}}}{\pi} + 1.405\left(\frac{\alpha_{\mathrm{s}}}{\pi}\right)^2 - 12.8\left(\frac{\alpha_{\mathrm{s}}}{\pi}\right)^3 - \frac{\alpha\alpha_{\mathrm{s}}Q^2_f}{4\pi^2}\,, \end{aligned} \tag{B.1}$$

with α and $\alpha_{\rm s}$ the electromagnetic and QCD constants, respectively. The values of α and $\alpha_{\rm s}$ are calculated at the $M_{Z'}$ scale as shown in (29) and (30), in agreement with each particle content and quark thresholds [46].

In order to calculate the running masses for all quarks, we should use the running QCD constant at the nth quark threshold [46], which is defined as

$$\alpha_{\rm s}^{(n)}(\mu)=\frac{4\pi}{\beta_0^{(n)}L^{(n)}}\left\{1-\frac{2\beta_1^{(n)}\ln[L^{(n)}]}{\left(\beta_0^{(n)}\right)^2L^{(n)}}+\frac{4\left(\beta_1^{(n)}\right)^2}{\left(\beta_0^{(n)}\right)^4(L^{(n)})^2}\times\left[\left(\ln(L^{(n)})-\frac{1}{2}\right)^2+\frac{\beta_0^{(n)}\beta_2^{(n)}}{8\left(\beta_1^{(n)}\right)^2}-\frac{5}{4}\right]\right\}, \quad \text{(B.2)}$$

with $L^{(n)}=\ln(\mu^2/(\Lambda^{(n)})^2)$, $\beta_0^{(n)}=11-(2/3)n_f$, $\beta_1^{(n)}=51-(19/3)n_f$, $\beta_2^{(n)}=2857-(5033/9)n_f+(325/27)n_f^2$, and n_f the number of quarks with mass less than μ. The asymptotic scale parameters $\Lambda^{(n)}$ for the energy scale μ at each quark threshold are determined by [58–60]

$$\begin{aligned}&2\beta_0^{(n-1)}\ln\left(\frac{\Lambda^{(n)}}{\Lambda^{(n-1)}}\right)\\&=\left(\beta_0^{(n)}-\beta_0^{(n-1)}\right)L^{(n)}+2\left(\frac{\beta_1^{(n)}}{\beta_0^{(n)}}-\frac{\beta_1^{(n-1)}}{\beta_0^{(n-1)}}\right)\ln(L^{(n)})\\&\quad-\frac{2\beta_1^{(n-1)}}{\beta_0^{(n-1)}}\ln\left(\frac{\beta_0^{(n)}}{\beta_0^{(n-1)}}\right)\\&\quad+\frac{4\beta_1^{(n)}}{\left(\beta_0^{(n)}\right)^2}\left(\frac{\beta_1^{(n)}}{\beta_0^{(n)}}-\frac{\beta_1^{(n-1)}}{\beta_0^{(n-1)}}\right)\frac{\ln(L^{(n)})}{L^{(n)}}\\&\quad+\frac{1}{\beta_0^{(n)}}\left[\left(\frac{2\beta_1^{(n)}}{\beta_0^{(n)}}\right)^2-\left(\frac{2\beta_1^{(n-1)}}{\beta_0^{(n-1)}}\right)^2\right.\\&\quad\left.-\frac{\beta_2^{(n)}}{2\beta_0^{(n)}}+\frac{\beta_2^{(n-1)}}{2\beta_0^{(n-1)}}-\frac{22}{9}\right]\frac{1}{L^{(n)}}\,,\end{aligned} \quad \text{(B.3)}$$

where the starting parameter is $\Lambda^{(5)}=217^{+25}_{-23}\,\text{MeV}$ [43]. We get for each threshold $\mu=m_q^{(n)}$ (with $n=3$ for the light quarks u,d,s below 1 GeV, and $n=4,5,6$, each one corresponding to the heavy quarks c, b and t, respectively)

$$\Lambda^{(3)}=342\,\text{MeV}\,;\quad \Lambda^{(4)}=301\,\text{MeV}\,;\quad \Lambda^{(6)}=91.7\,\text{MeV}\,. \quad \text{(B.4)}$$

The running mass for the heavy quarks $q=c,b,t$ at $\mu<\mu^{n+1}$ is

$$\bar{m}_{qn}(\mu)=\frac{R^{(n)}(\mu)}{R^{(n)}(m^{\rm pole})}m_q^{\rm pole}, \quad \text{(B.5)}$$

while for the light quarks $q=u,d,s$ is

$$\bar{m}_q(\mu)=\frac{R^{(3)}(\mu)}{R^{(3)}(1\,\text{GeV})}m_q(1\,\text{GeV})\,, \quad \text{(B.6)}$$

where the $m_q^{\rm pole}$ are the pole masses and the $m_q(1\,\text{GeV})$ are the masses measured at the 1 GeV scale. We use the following values [46]:

$$\begin{aligned}m_c^{\rm pole}&=1.26\pm0.13\,\text{GeV}\,,\\m_b^{\rm pole}&=4.26\pm0.15\,\text{GeV}\,,\\m_t^{\rm pole}&=174.3\pm5.1\,\text{GeV}\,,\\m_u(1\,\text{GeV})&=4.88\pm0.57\,\text{MeV}\,,\\m_d(1\,\text{GeV})&=9.81\pm0.65\,\text{MeV}\,,\\m_s(1\,\text{GeV})&=195.4\pm12.5\,\text{MeV}\,.\end{aligned} \quad \text{(B.7)}$$

We also use

$$\begin{aligned}R^{(n)}(\mu)=\left(\frac{\beta_0\alpha_{\rm s}^{(n)}}{2\pi}\right)^{2\gamma_0/\beta_0}&\left\{1+\left[\frac{2\gamma_1}{\beta_0}-\frac{\beta_1\gamma_0}{\beta_0^2}\right]\frac{\alpha_{\rm s}^{(n)}}{\pi}\right.\\&+\frac{1}{2}\left[\left(\frac{2\gamma_1}{\beta_0}-\frac{\beta_1\gamma_0}{\beta_0^2}\right)^2+\frac{2\gamma_2}{\beta_0}-\frac{\beta_1\gamma_1}{\beta_0^2}\right.\\&\left.\left.-\frac{\beta_2\gamma_0}{16\beta_0^2}+\frac{\beta_1^2\gamma_0}{2\beta_0^3}\right]\left(\frac{\alpha_{\rm s}^{(n)}}{\pi}\right)^2\right\},\end{aligned} \quad \text{(B.8)}$$

with $\gamma_0=2$, $\gamma_1=\frac{101}{12}-\frac{5}{18}n_f$, and $\gamma_2=\frac{1}{32}\big[1249-\big(\frac{2216}{27}+\frac{160}{3}\zeta(3)\big)n_f-\frac{140}{81}n_f^2\big]$. In order to get the running mass at $\mu=M_{Z_2}>\mu^{(6)}=m_t$, it is necessary to use the matching condition [58–60]

$$\begin{aligned}\bar{m}_{qn}^{(N)}(\mu)=\bar{m}_{qn}^{(N-1)}(\mu)&\\\times\left[1+\frac{1}{12}\left(x_N^2+\frac{5}{3}x_N+\frac{89}{36}\right)\left(\frac{\alpha_{\rm s}^{(N)}}{\pi}\right)^2\right]^{-1},&\end{aligned} \quad \text{(B.9)}$$

where $x_N=\ln[(m_{q_N}^{(N)}/\mu)^2]$, $N>n$, and $\mu_N\le\mu\le\mu_{N+1}$. By iterating the above equation, along with the definitions (B.5) and (B.6), at each quark threshold, we obtain the values given by (20) and the value of $\alpha_{\rm s}^{(6)}=\alpha_{\rm s}(Z')$ in (29) for the extended dilepton model.

On the other hand, for the MEDM in Sects. 2.4 and 3.2, we have a new threshold at $\mu=m_J^{(n)}=3\,\text{TeV}$ with $n=7$ associated with the exotic quarks of the minimal model. The asymptotic scale parameter $\Lambda^{(7)}$ at this new quark threshold is obtained from (B.3) with $\Lambda^{(6)}$ given in (B.4), from which $\Lambda^{(7)}=24.8\,\text{MeV}$. In this case, the running top mass at $\mu=M_{Z'}>\mu^{(7)}=m_J$ can be obtained from (B.9) with $N=7$, $q_n=t$, $x_7=\ln[(m_J^{(7)}/\mu)^2]$ and $m_J^{(7)}=m_J=3\,\text{TeV}$, and we obtain the value $\bar{m}_t(4\,\text{TeV})=142.579\,\text{GeV}$ in (20) for the MEDM. The QCD constant in this case runs as (B.2), but with $n=7$ at the Z' scale, leading to the value of $\alpha_{\rm s}(Z')$ in (30) for the MEDM.

References

1. J.S. Bell, R. Jackiw, Nuovo Cim. A **60**, 47 (1969)
2. S.L. Adler, Phys. Rev. **177**, 2426 (1969)
3. D.J. Gross, R. Jackiw, Phys. Rev. D **6**, 477 (1972)
4. H. Georgi, S.L. Glashow, Phys. Rev. D **6**, 429 (1972)
5. S. Okubo, Phys. Rev. D **16**, 3528 (1977)
6. J. Banks, H. Georgi, Phys. Rev. **14**, 1159 (1976)

7. S. Godfrey, in: Proc. of the APS/DPF/DPB Summer Study on the Future of Particles Physics, Snowmass, 2001, ed. by N. Graf [hep-ph/0201093, hep-ph/0201092]
8. M. Carena, A. Daleo, B.A. Dobrescu, T.M.P. Tait, Phys. Rev. D **70**, 093 009 (2004)
9. LHC/LC Study Group, G. Weiglein et al., hep-ph/0410364
10. P.H. Frampton, P.Q. Hung, M. Sher, hep-ph/9903387 v2
11. C.A. de S. Pires, O.P. Ravinez, Phys. Rev. D **58**, 35 008 (1998)
12. C.A. de S. Pires, Phys. Rev. D **60**, 075 013 (1999)
13. L.A. Sánchez, W.A. Ponce, R. Martínez, Phys. Rev. D **64**, 075 013 (2001)
14. R. Foot, H.N. Long, T.A. Tran, Phys. Rev. D **50**, R34 (1994)
15. H.N. Long, Phys. Rev. D **53**, 437 (1996)
16. H.N. Long, Phys. Rev. D **54**, 4691 (1996)
17. H.N. Long, Mod. Phys. Lett. A **13**, 1865 (1998)
18. F. Pisano, V. Pleitez, Phys. Rev. D **46**, 410 (1992)
19. P.H. Frampton, Phys. Rev. Lett. **69**, 2889 (1992)
20. P.H. Frampton, P. Krastev, J.T. Liu, Mod. Phys. Lett. A **9**, 761 (1994)
21. P.H. Frampton et al., Mod. Phys. Lett. A **9**, 1975 (1994)
22. T.A. Nguyen, A.K. Nguyen, N.L. Hoang, Int. J. Mod. Phys. A **16**, 541 (2001)
23. R.A. Diaz, R. Martinez, F. Ochoa, Phys. Rev. D **69**, 095 009 (2004)
24. R.A. Diaz, R. Martinez, F. Ochoa, Phys. Rev. D **72**, 035 018 (2005)
25. F. Ochoa, R. Martinez, Phys. Rev. D **72**, 035 010 (2005)
26. A.G. Dias, R. Martínez, V. Pleitez, Eur. Phys. J. C **39**, 101 (2005)
27. A.G. Dias, Phys. Rev. D **71**, 015 009 (2005)
28. G.A. González-Sprinberg, R. Martínez, O. Sampayo, Phys. Rev. D **71**, 115 003 (2005)
29. K.T. Mahanthappa, P.K. Mohapatra, Phys. Rev. D **42**, 1732 (1990)
30. K.T. Mahanthappa, P.K. Mohapatra, Phys. Rev. D **43**, 3093 (1991)
31. A. Carcamo, R. Martinez, F. Ochoa, Phys. Rev. D **73**, 035 007 (2006)
32. J. Gunion et al., in: The Higgs Hunter's Guide (Addison-Wesley, New York, 1990)
33. S. Glashow, S. Weinberg, Phys. Rev. D **15**, 1958 (1977)
34. D. Atwood, L. Reina, A. Soni, Phys. Rev. Lett. **75**, 3800 (1993)
35. D. Atwood, L. Reina, A. Soni, Phys. Rev. D **53**, 1199 (1996)
36. D. Atwood, L. Reina, A. Soni, Phys. Rev. D **54**, 3296 (1996)
37. D. Atwood, L. Reina, A. Soni, Phys. Rev. D **55**, 3156 (1997)
38. M. Sher, Yao Yuan, Phys. Rev. D **44**, 1461 (1991)
39. T.P. Cheng, M. Sher, Phys. Rev. D **35**, 3490 (1987)
40. K. Matsuda, H. Nishiura, Phys. Rev. D **69**, 053 005 (2004)
41. D.G. Dumm, F. Pisano, V. Pleitez, Mod. Phys. Lett. A **9**, 1609 (1994)
42. C. Promberger, S. Schatt, F. Schwab, hep-ph/0702169 (2007)
43. Particle Data Group, S. Eidelman et al., Phys. Lett. B **592**, 120 (2004)
44. J. Bernabeu, A. Pich, A. Santamaria, Nucl. Phys. B **363**, 326 (1991)
45. D. Bardin et al., Electroweak Working Group Report, hep-ph/9709229 (1997) pp. 28–32
46. H. Fusaoka, Y. Koide, Phys. Rev. D **57**, 3986 (1998)
47. M.A. Perez, G. Tavares-Velasco, J.J. Toscano, Phys. Rev. D **69**, 115 004 (2004)
48. M.A. Perez, M.A. Soriano, Phys. Rev. D **46**, 125 (1992)
49. A. Ghosal, Y. Koide, H. Fusaoka, Phys. Rev. D **64**, 053 012 (2001)
50. J.I. Illana, T. Riemann, Phys. Rev. D **63**, 053 004 (2001)
51. D. Delepine, F. Vissani, Phys. Lett. B **522**, 95 (2001)
52. T. Rador, Phys. Rev. D **59**, 095 012 (1999)
53. P. Langacker, M. Plumacher, Phys. Rev. D **62**, 013 006 (2000)
54. V. Barger, C.-W. Chiang, P. Langacker, H.-S. Lee, Phys. Lett. B **580**, 186 (2004)
55. S. Fajfer, P. Singer, Phys. Rev. D **65**, 017 301 (2002)
56. D.L. Anderson, M. Sher, Phys. Rev. D **72**, 095 014 (2005)
57. J.A. Rodriguez, M. Sher, Phys. Rev. D **70**, 117 702 (2004)
58. W. Bernreuther, W. Wetzel, Nucl. Phys. B **197**, 228 (1982)
59. W. Bernreuther, Ann. Phys. **151**, 127 (1983)
60. K.G. Chetyrkin, B.A. Kniehl, M. Steinhauser, Phys. Rev. Lett. **79**, 2184 (1997)